HHS Public Access

Author manuscript

Curr Opin Chem Biol. Author manuscript; available in PMC 2021 April 01.

Published in final edited form as:

Curr Opin Chem Biol. 2020 April ; 55: 19–25. doi:10.1016/j.cbpa.2019.12.002.

Advances in visualization of copper in mammalian systems using X-ray fluorescence microscopy

Scot C. Leary[1], **Martina Ralle**[2]

[1]Department of Biochemistry, Microbiology and Immunology, University of Saskatchewan, Saskatoon, Saskatchewan 7N 5E5, Canada.

[2]Department of Molecular and Medical Genetics, Oregon Health & Science University, Portland, Oregon, United States

Abstract

Synchrotron-based X-ray fluorescence microscopy (XFM) has become an important imaging technique to investigate elemental concentrations and distributions in biological specimens. Advances in technology now permit imaging at resolutions rivaling that of electron microscopy, and researchers can now visualize elemental concentrations in subcellular organelles when using appropriate correlative methods. XFM is an especially valuable tool to determine the distribution of endogenous trace metals that are involved in neurodegenerative diseases. Here, we discuss the latest research on the unusual copper (Cu) storage vesicles that were originally identified in mouse brains and the involvement of Cu in Alzheimer's disease. Lastly, we provide an outlook of how future improvements to XFM will drive current trace element research forward.

Keywords

X-ray fluorescence microscopy; copper storage vesicles; copper dyshomeostasis in Alzheimer's disease

1. Introduction

Synchrotron-based x-ray fluorescence microscopy (XFM) is a robust technique to quantitatively determine the distribution of trace elements like metals in a biological specimen with high sensitivity and, if needed, high resolution. The method does not require dyes or other labeling steps because detection of each element is based on its intrinsic fluorescence properties (i.e. photoelectric effect). XFM therefore allows one to directly quantify the abundance of a specific element. Samples are raster scanned through a focused

Corresponding author, Ralle, Martina (rallem@ohsu.edu).

Declaration of interests

The authors declare that they have no known competing financial interests or personal relationships that could have appeared to influence the work reported in this paper.

x-ray beam in an x/y pattern and two-dimensional elemental distributions are produced from the emitted fluorescence spectra at each pixel (Figure 1).

Typically, x-rays fully penetrate biological samples (> 10 μm) and elemental concentrations can be calculated in three dimensions if the thickness of the specimen is known. Because biological material is almost transparent to high energy x-rays (weak absorption contrast), highly brilliant x-ray sources are needed to produce a detectable x-ray fluorescence response signal over a micro to nanometer scale. As a consequence, XFM experiments on biological samples requiring micron to submicron resolution are usually carried out at synchrotron sources, though commercial benchtop instruments like the Sigray AttoMap Micro XRF are rapidly improving in performance and resolution (<8 μm).

XFM and its related applications have enabled the research community to obtain rich information about the distribution and speciation of elements in organs, tissues and cells (Figure 1). In fact, over the past two decades the use of biological XFM has expanded from ‘exploratory’ elemental imaging [2] to include narrowly focused investigations of the distribution and speciation of platinum in tumor cells [3] or iron (Fe) in hemozoin deposits in mouse macrophages [4]. XFM has also been invaluable to studies of copper (Cu) that identified unexpected and highly concentrated Cu pools within biological systems (Figure 1 and [5]), contributed to a better understanding of disease processes associated with impaired Cu handling [6] and facilitated targeted development of therapies for Cu handling disorders [*7]. These advances are in part attributable to improvements in focusing optics (decreased spot size and increased photon yield), energy dispersive detector technologies (increased energy resolution), read-out electronics (increase of maximum number of photons processed per second) and data acquisition software. This review will focus on how XFM has advanced our understanding of Cu homeostasis in the brain and how it has begun to illuminate the role of Cu in neurodegenerative diseases over the past 3 years.

2. Cu storage vesicles (CSVs) in mammals

Work by Pushkar and colleagues previously showed that Cu accumulates to high concentrations in small puncta termed CSVs in astrocytes within the periventricular region of the lateral ventricle in rat and mouse brains [5]. Cu levels within CSVs were found to exceed 100 mM, a concentration that is cytotoxic when used in cell culture. We detected the same Cu foci around all ventricles of the mouse brain (Figure 1) and, upon investigating the development of these CSVs in greater detail, found that they grow deeper into the brain parenchyma (interstitium) with age (Figure 2). Our current hypothesis is that these CSVs act as a ‘filter’ to tightly control the Cu content of the interstitial fluid that is available to neurons. The majority of Cu entering the brain traverses the cells of the choroid plexus and passes into the cerebral spinal fluid (CSF), which then freely diffuses through the ependymal layer of the ventricles into the brain parenchyma and becomes interstitial fluid [9]. Elevated Cu concentrations in the CSF will thus be buffered by what may be specialized astrocytes, which import Cu with high affinity and store it within CSVs. The importance of balancing the Cu concentration in interstitial fluid was underscored by a remarkable high resolution study from Perrin and colleagues in primary rat hippocampal neurons [10]. The authors showed how local Cu and zinc (Zn) distributions were fundamental for tubulin- and actin-

dependent stability of dendrites. XFM scans at 20 nm resolution localized to dendritic spines suggested that either Cu chelation or supplementation at sub-cytotoxic concentrations leads to reduced F-actin and β-tubulin levels, albeit via different mechanisms.

Fu et al. showed previously that the levels of metallothioneins (MT) 1/2 and 3 were dramatically increased in the ventricular zone of rats as they aged [11]. An XFM study by Sullivan et al. found that the number of CSVs, but not their Cu content, was decreased in MT1/2 knockout mice [*12]. MT1/2 knockout mice also exhibited a decrease in basal Cu in the periventricular region, which led the authors to echo Fu et al. and suggest that all three MT isoforms are involved in the formation and/or maintenance of CSVs (Figure 3a). In MT1/2 knockout mice one would predict that basal Cu storage capacity is lower and fewer Cu loaded MTs are available to form CSVs because MT3 expression is not induced by Cu or Zn and is thus unlikely to compensate for loss of MT1/2 function. In contrast, we expected CSV numbers and Cu content to be unchanged in MT3 single knockout mice when compared to controls because Cu upregulates MT1/2 expression, yet our XFM studies found instead that deletion of MT3 or MT1/2 had comparable consequences on CSV dynamics (Figure 4, unpublished). The fact that MT1/2 did not compensate for the lack of MT3 function suggests an alternative, MT-independent pathway for the formation and regulation of CSVs (Figure 3b,c). In this model, some Cu would still be sequestered by MTs but Cu chaperones like Atox1 or high affinity Cu binding peptides like GSH would transport Cu to vesicles (possibly lysosomes or late endosomes). Cu would then either be actively (via a transporter) or passively (via autophagy) transferred into CSVs. Upon deletion of either MT isoform, cytosolic Cu content is decreased and less Cu is available to populate CSVs owing to reduced expression of the Cu import protein Ctr1 or increased Cu export activity. Insight into how Cu export from CSVs is blocked was provided by work from Ohrvik and colleagues who showed that CSVs are formed throughout mouse brains lacking Ctr2, a mammalian Cu transporter that assists in liberating Cu from transiently formed storage vesicles [14]. Therefore, an attractive hypothesis is that Ctr2 is inactivated in specialized astrocytes harboring CSVs (Figure 3a–c).

Further studies that characterize the regulation of CSV dynamics in mammals may inform us as to how to direct Cu to form CSVs. Such advances in turn would offer new therapeutic avenues for the treatment of Cu overload disorders like Wilson disease where blocked Cu export leads to uncontrolled cellular Cu accumulation and results in aberrant regulation of several important homeostatic processes.

3 Alzheimer’s Disease

Dyshomeostasis of transition metals as a contributing factor to Alzheimer’s disease (AD) was suggested as early as 1953 [15]. In 2000, a widely cited paper by A. Bush claimed a ‘consensus’ view of elevated levels of Fe, Cu and Zn levels in AD brain [16]. Subsequent meta-analysis by Schrag et al. [17] and bulk quantitative analysis of these elements in AD patient brains and controls decisively debunked this claim [18]. In fact, it was shown that Cu levels were lower in AD brains, while Fe and Zn concentrations were elevated and unchanged respectively. In recent years, transition metal studies in AD have focused on further characterizing Aβ plaque pathology and investigating a possible role of transition

metal chemistry. Using correlative XFM and IR spectroscopy, Leskovjan and colleagues reported increased Zn levels in Aβ plaques in a mouse model of AD that overexpresses human presenilin and a chimeric amyloid precursor protein (PSAPP) [19]. Interestingly, PSAPP mice did not show an elevation of Fe or Cu in plaques while Fe was increased in the brain parenchyma. It was later shown that in mouse models presenting with severe neurodegeneration (5 × FAD and CVN), Cu but not Fe was increased in Aβ plaques [20]. The authors concluded that Cu accumulation in Aβ plaques is correlated with the degree of neurodegeneration.

James et al. published a follow-up report in which they used the powerful Maia detector at the Australian synchrotron to analyze 49 plaques from 4 PSAPP animals for their metal content (previous studies analyzed <10 plaques). Instead of employing a correlative approach they used Compton scattering to identify plaques. Their findings mirrored those of Leskovjan et al. with Aβ plaques having less Fe compared to the surrounding neuropil, insignificant changes in Cu levels and increased Zn levels when concentrations were normalized to plaque density (i.e. proteinacous content) [21]. The authors concluded that concentrations of Cu and Zn within Aβ plaques is dependent on the levels of these metals in the surrounding neuropil. Having established that plaques may contain more Cu, it is now crucial to understand how Cu promotes the oligomerization of Aβ peptides and the formation of β amyloid fibrils. Summers and colleagues took the first step towards this end by showing that the Cu(II) - Aβ(1–42) coordination of monomeric Aβ(1–42) in solution depends on pH and other stabilizing compounds added to the solution [22]. XANES and EXAFS investigations of the bulk material revealed a square planar O/N Cu(II) environment at pH 6.1 and 7.4, while the Cu(II) coordination changed to a square pyramidal geometry at pH 9.0. Based on their own work and that of others, the authors suggested that Cu(II) binding to Aβ peptides exists in several different confirmations in vivo and may include some unspecific binding. Future studies that employ time-resolved Cu k-edge EXAFS analysis of the oligomerization process and EXAFS analysis of β amyloid fibrils may shed further light on this issue.

4. Current challenges and future developments

With the highest sensitivity to date and resolutions approaching the low nanometer range, a new limitation of XFM has surfaced. The only information XFM provides is the elemental distribution, making it impossible to detect cellular or subcellular structures unless they exhibit significant differences in elemental concentrations (e.g. phosphorous in the nucleus). Thus, several laboratories are actively developing correlative approaches to directly detect trace element distribution in (sub)cellular structures. These include the parallel use of synchrotron-based ptychography, multipronged microscopy approaches and gene editing methods that incorporate an XFM-detectable tag into the desired gene of a model organism [**23–26]. A particularly nice albeit extremely challenging example of a correlative approach using epifluorescence was provided by Carmona and colleagues who showed that feeding manganese (Mn) to HeLa cells lacking the wild-type Mn transporter SLC30A10 leads to Mn accumulation in the trans-Golgi network. RFP constructs were used to visualize the Golgi in HeLa cells alone or in those transfected with cDNAs encoding wild-type or disease-causing variants of *SLC30A10*. Once visualized by epifluorescence, HeLa cells

were flash frozen and scanned for their elemental distributions allowing for the overlay of Mn and SLC30A10 profiles [*27].

Upgrades to 4th generation synchrotron sources are currently underway (ESRF) or planned (APS) and will improve brilliance, coherence and further decrease pulse duration of synchrotron x-rays by 100 – 1000-fold. For users with biological or biomedical interests, these upgrades will greatly increase throughput (scan times will also be 100x −1000x faster) regardless of the resolution. Thus, collection of statistical data for biological replicates will be possible and 3D-tomography will become routine. The number of high-resolution studies is expected to increase and with correlative methods in place researchers will be able to ask new scientific questions. Direct co-localization of proteins and metals will provide further insights into metal homeostasis in complex biological specimens where bulk methods fail. For example, an important finding by the Lutsenko group described distinct distribution patterns of the Cu transporter Atp7b and Cu in the crypts of the small intestine, which may have important implications for Cu uptake into the lumen [28]. Once high-resolution and correlative methods are in hand it will be possible to simultaneously detect Cu and Atp7b in a single XFM scan.

In summary, XFM is a reliable tool to solve scientific questions that involve trace metals. Progress in technique development that is expected over the next decade will further enhance the capabilities and transform XFM into a routine analysis tool.

Acknowledgments

Funding

This research was supported by grant-in-aid of research from the Canadian Institutes of Health Research (MOP#133562) to S.L. and by the National Institute of General Medicine (GM129592, GM090016) to M.R. The Advanced Photon Source at Argonne National Laboratory was supported by the U.S. Department of Energy, Office of Science, Office of Basic Energy Sciences under contract DE-AC02–06CH11357

Abbreviations

XFM	x-ray fluorescence microscopy
CSF	cerebral spinal fluid
CSV	copper storage vesicles
MT	metallothionein
AD	Alzheimer’s disease
ESRF	European synchrotron radiation facility
APS	Advanced Photon Source, Argonne National Laboratory, IL
XANES	X-ray absorption near edge spectroscopy
EXAFS	extended x-ray absorption fine spectrum

References

1. Vogt S: Maps: A set of software tools for analysis and visualization of 3D X-ray fluorescent datasets. Journal De Physique IV 2003, 104:635–638.
2. Twining BS, Baines SB, Fisher NS, Maser J, Vogt S, Jacobsen C, Tovar-Sanchez A, Sañudo-Wilhelmy SA: Quantifying trace elements in individual aquatic protist cells with a synchrotron x-ray fluorescence microprobe. Analytical Chemistry 2003, 75:3806–3816. [PubMed: 14572047]
3. Popovic J, Klajn A, Paunesku T, Ma Q, Chen S, Lai B, Stevanovic M, Woloschak GE: Neuroprotective role of selected antioxidant agents in preventing cisplatin-induced damage of human neurons in vitro. Cell Mol Neurobiol 2019, 39:619–636. [PubMed: 30874981]
4. Pek RH, Yuan X, Rietzschel N, Zhang J, Jackson L, Nishibori E, Ribeiro A, Simmons W, Jagadeesh J, Sugimoto H, et al.: Hemozoin produced by mammals confers heme tolerance. eLife 2019, 8:e49503. [PubMed: 31571584]
5. Pushkar Y, Robison G, Sullivan B, Zheng W, Fu SX, Kohne M, Jiang W, Rohr S, Lai B, Marcus MA, et al.: Aging results in copper accumulations in GFAP-positive cells in the subventricular zone. Aging Cell 2013.
6. Ralle M, Huster D, Vogt S, Schirrmeister W, Burkhead JL, Capps TR, Gray L, Lai B, Maryon E, Lutsenko S: Wilson's disease at a single cell level:intracellular copper trafficking activates compartment-specific responses in hepatocytes. J Biol Chem 2010.
7. Haddad MR, Choi EY, Zerfas PM, Yi L, Martinelli D, Sullivan P, Goldstein DS, Centeno JA, Brinster LR, Ralle M, et al.: Cerebrospinal fluid-directed raav9-rsatp7a plus subcutaneous copper histidinate advance survival and outcomes in a menkes disease mouse model. Mol Ther Methods Clin Dev 2018, 10:165–178. [PubMed: 30090842] * The authors successfully developed a gene therapy method in combination with Cu injections to slow Menkes disease in a mouse model. XFM clearly showed restoration of Cu levels in the brains of these mice.
8. Schneider CA, Rasband WS, Eliceiri KW: NIH Image to ImageJ: 25 years of image analysis. Nature Methods 2012, 9:671–675. [PubMed: 22930834]
9. Donsante A, Johnson P, Jansen LA, Kaler SG: Somatic mosaicism in Menkes disease suggests choroid plexus-mediated copper transport to the developing brain. Am J Med Genet A 2010, 152A:2529–2534. [PubMed: 20799318]
10. Perrin L, Roudeau S, Carmona A, Domart F, Petersen JD, Bohic S, Yang Y, Cloetens P, Ortega R: Zinc and copper effects on stability of tubulin and actin networks in dendrites and spines of hippocampal neurons. ACS Chemical Neuroscience 2017, 8:1490–1499. [PubMed: 28323401]
11. Fu S, Jiang W, Zheng W: Age-dependent increase of brain copper levels and expressions of copper regulatory proteins in the subventricular zone and choroid plexus. Frontiers in Molecular Neuroscience 2015, 8.
12. Sullivan B, Robison G, Osborn J, Kay M, Thompson P, Davis K, Zakharova T, Antipova O, Pushkar Y: On the nature of the Cu-rich aggregates in brain astrocytes. Redox Biology 2017, 11:231–239. [PubMed: 28012438] * This study filled an important gap in our knowledge about CSVs. The authors were able to demonstrate that CSVs were formed even in the absence of MT1/2 using XFM.
13. Lee SJ, Koh JY: Roles of zinc and metallothionein-3 in oxidative stress-induced lysosomal dysfunction, cell death, and autophagy in neurons and astrocytes. Mol Brain 2010, 3:30. [PubMed: 20974010]
14. Ohrvik H, Nose Y, Wood LK, Kim BE, Gleber SC, Ralle M, Thiele DJ: Ctr2 regulates biogenesis of a cleaved form of mammalian Ctr1 metal transporter lacking the copper- and cisplatin-binding ecto-domain. Proc Natl Acad Sci U S A 2013, 110:E4279–4288. [PubMed: 24167251]
15. GOODMAN L: Alzheimer's disease: A clinico-pathologic analysis of twenty-three cases with a theory on pathogenesis. The Journal of Nervous and Mental Disease 1953, 118:97–130. [PubMed: 13109530]
16. Bush AI: Metals and neuroscience. Curr Opin Chem Biol 2000, 4:184–191. [PubMed: 10742195]
17. Schrag M, Mueller C, Oyoyo U, Smith MA, Kirsch WM: Iron, zinc and copper in the alzheimer's disease brain: a quantitative meta-analysis. some insight on the influence of citation bias on scientific opinion. Prog Neurobiol 2011,94:296–306. [PubMed: 21600264]

18. Graham SF, Nasaruddin MB, Carey M, Holscher C, McGuinness B, Kehoe PG, Love S, Passmore P, Elliott CT, Meharg AA, et al.: Age-associated changes of brain copper, iron, and zinc in Alzheimer's disease and dementia with Lewy bodies. J Alzheimers Dis 2014, 42:1407–1413. [PubMed: 25024342]

19. Leskovjan AC, Kretlow A, Lanzirotti A, Barrea R, Vogt S, Miller LM: Increased brain iron coincides with early plaque formation in a mouse model of Alzheimer's disease. Neuroimage 2011, 55:32–38. [PubMed: 21126592]

20. Bourassa MW, Leskovjan AC, Tappero RV, Farquhar ER, Colton CA, Van Nostrand WE, Miller LM: Elevated copper in the amyloid plaques and iron in the cortex are observed in mouse models of Alzheimer's disease that exhibit neurodegeneration. Biomedical spectroscopy and imaging 2013, 2:129–139. [PubMed: 24926425]

21. James SA, Churches QI, de Jonge MD, Birchall IE, Streltsov V, McColl G, Adlard PA, Hare DJ: Iron, copper, and zinc concentration in abeta plaques in the app/ps1 mouse model of alzheimer's disease correlates with metal levels in the surrounding neuropil. ACS Chem Neurosci 2017, 8:629–637. [PubMed: 27958708]

22. Summers KL, Schilling KM, Roseman G, Markham KA, Dolgova NV, Kroll T, Sokaras D, Millhauser GL, Pickering IJ, George GN: X-ray Absorption Spectroscopy Investigations of Copper(II) Coordination in the Human Amyloid beta Peptide. Inorg Chem 2019, 58:6294–6311. [PubMed: 31013069]

23. Deng J, Lo YH, Gallagher-Jones M, Chen S, Pryor A, Jin Q, Hong YP, Nashed YSG, Vogt S, Miao J, et al.: Correlative 3D x-ray fluorescence and ptychographic tomography of frozen-hydrated green algae. Science Advances 2018, 4:eaau4548. [PubMed: 30406204] ** This paper describes how ptychography and XFM can be used correlatively to determine elemental distributions in subcellular organelles. This will be one of the methods used in the future to identify subcellular structures when conducting XFM experiments

24. Ducic T, Stamenkovic S, Lai B, Andjus P, Lucie V: Multimodal Synchrotron Radiation Microscopy of Intact Astrocytes from the hSOD1 G93A Rat Model of Amyotrophic Lateral Sclerosis. Analytical Chemistry 2019, 91:1460–1471. [PubMed: 30571081]

25. Genoud S, Roberts BR, Gunn AP, Halliday GM, Lewis SJG, Ball HJ, Hare DJ, Double KL: Subcellular compartmentalisation of copper, iron, manganese, and zinc in the Parkinson's disease brain. Metallomics 2017, 9:1447–1455. [PubMed: 28944802]

26. Victor TW, Easthon LM, Ge M, O'Toole KH, Smith RJ, Huang X, Yan H, Allen KN, Chu YS, Miller LM: X-ray Fluorescence Nanotomography of Single Bacteria with a Sub-15 nm Beam. Sci Rep 2018, 8:13415. [PubMed: 30194316]

27. Carmona A, Zogzas CE, Roudeau S, Porcaro F, Garrevoet J, Spiers KM, Salome M, Cloetens P, Mukhopadhyay S, Ortega R: SLC30A10 Mutation Involved in Parkinsonism Results in Manganese Accumulation within Nanovesicles of the Golgi Apparatus. ACS Chem Neurosci 2019, 10:599–609. [PubMed: 30272946] * Using XFM at different resolutions, the authors convincingly demonstrate suborganelle accumulation of Mn. The authors sucessfully used correlative visual light microscopy and XFM to directly detect Mn in the Golgi network

28. Pierson H, Muchenditsi A, Kim BE, Ralle M, Zachos N, Huster D, Lutsenko S: The Function of ATPase Copper Transporter ATP7B in Intestine. Gastroenterology 2018, 154:168–180 e165. [PubMed: 28958857]

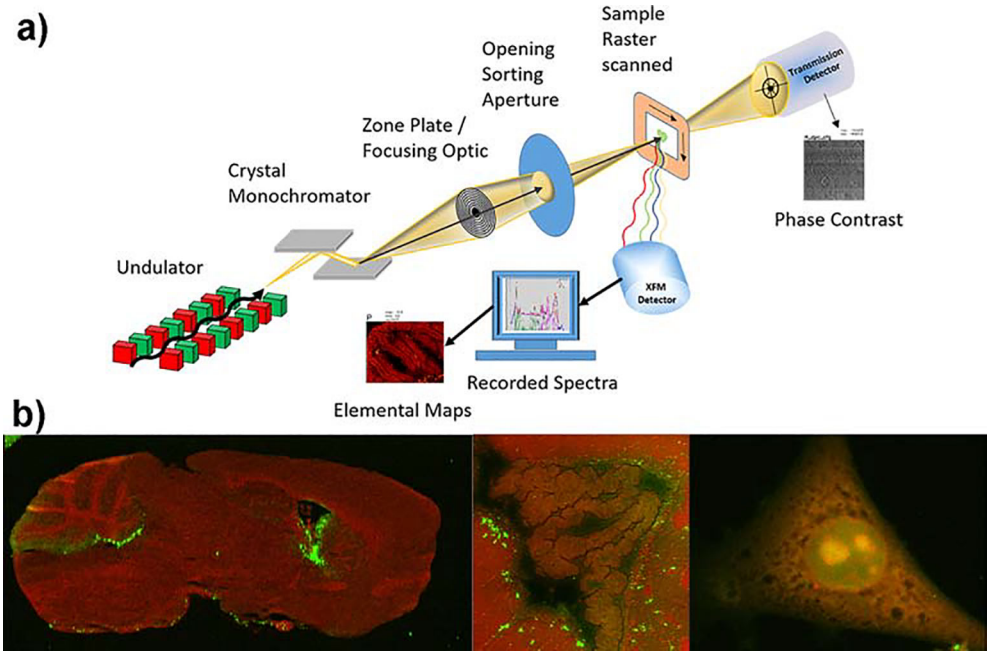

Figure 1. Principal experimental setup of XFM and representative elemental images.

a) A typical experimental setup for XFM is shown utilizing an undulator as a source for x-rays and a double crystal monochromator to tune the energy of the x-ray. A sample is scanned in x-y through the focused x-rays and fluorescence photons are collected by an energy dispersive detector. The spectra are fitted at each point and converted into area concentrations via calibration. b) Phosphorus (P, red) and Cu (green) co-localization maps of a saggital mouse brain section (left, 25 μm spot size), lateral ventricle of a coronal mouse brain section (middle, 2 μm spot size) and mouse embryonic fibroblast (right, 200 nm spot size). Elemental maps were created with the program MAPS [1]. Elemental concentration ranges are represented by false coloring from darkest (lowest concentration) to lightest (highest concentration). Mouse brain were provided by Dr. S. Hayflick (Oregon Health and Science University) and Dr. M. Knutson (University of Florida). Mouse embryonic fibroblasts were provided by Dr. M Petris (University of Missouri). Unpublished results.

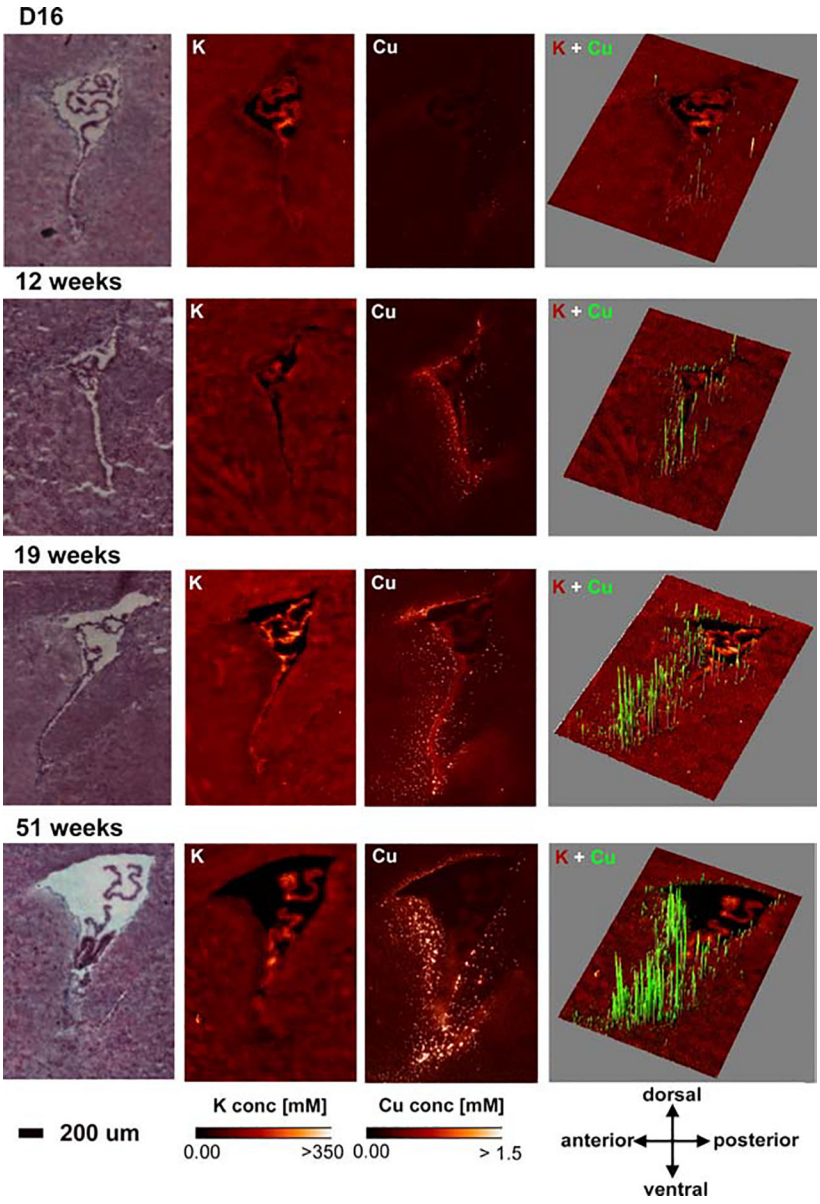

Figure 2. Age-dependent Cu accumulation into CSVs.

H&E images, elemental maps for potassium (K) and Cu, and 3D overlays for Cu (green) onto the K (red) maps are shown in brain at 16 days (D16), 12 weeks, 19 weeks and 51 weeks of age. Cu CSVs become more abundant and expand more into the brain parenchyma with age. Area concentration ranges for Cu in 3D maps were adjusted to maximize visualization (D16 0 -> 0.28 μg/cm^2, 12 weeks 0->1 μg/cm^2, 19 weeks 0->1.8 μg/cm^2, 51 weeks 0 -> 3.5 μg/cm^2). Elemental Maps were created with MAPS [1] and 3D overlays were created with the ImageJ 3D plugin [8]. Elemental concentration ranges are represented by false coloring from darkest (lowest concentration) to lightest (highest concentration). Mouse brains were provided by Dr. S. Hayflick (Oregon Health & Science University). Unpublished results.

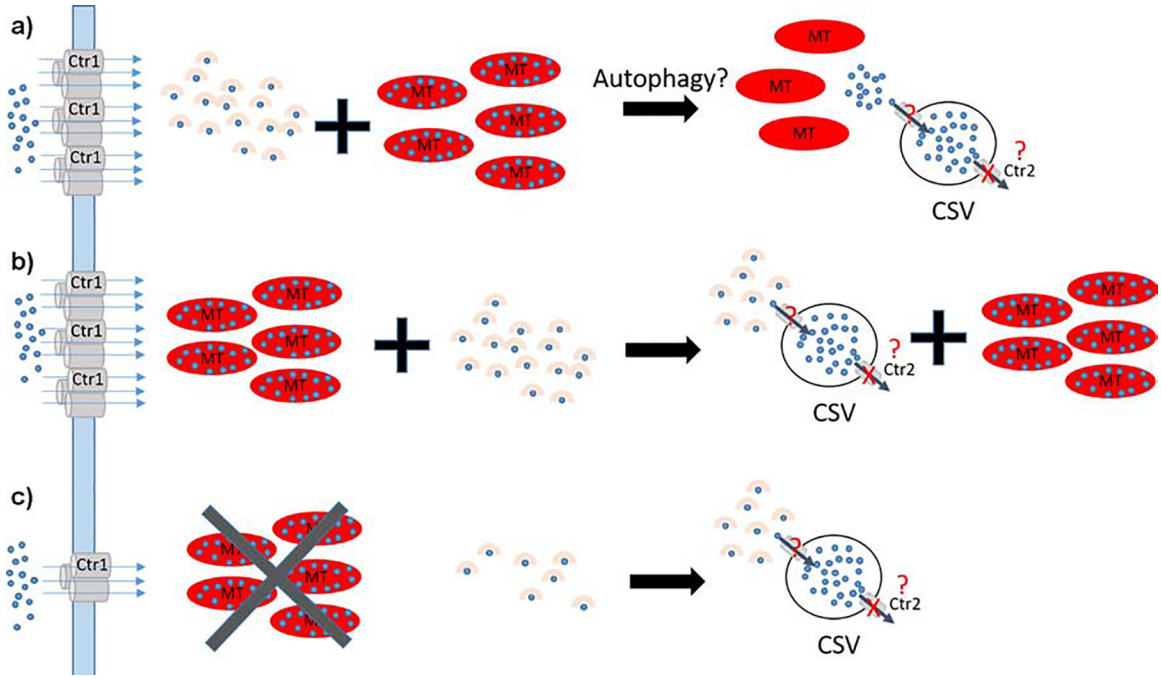

Figure 3. Possible models of CSV formation.

a) Model 1: Imported Cu (blue) is bound by chaperones or high affinity peptides (beige) delivered to target proteins or stored by MTs (red ovals). CSVs may be formed as a consequence of autophagy that initiates Cu release from MT and subsequent import into CSVs resembling what was described for MT3 [13]. Export is blocked because no Ctr2 is present. b) Model 2: In contrast to a) CSVs are populated by Cu from Cu chaperones or Cu-bound peptides. c) CSV formation in MT knockout brains. Model 2 can explain our XFM observations: MT knockouts reduce the cellular Cu storage capacity and signal for reduced Ctr1 expression at the plasma membrane. CSVs are populated with Cu as described in b).

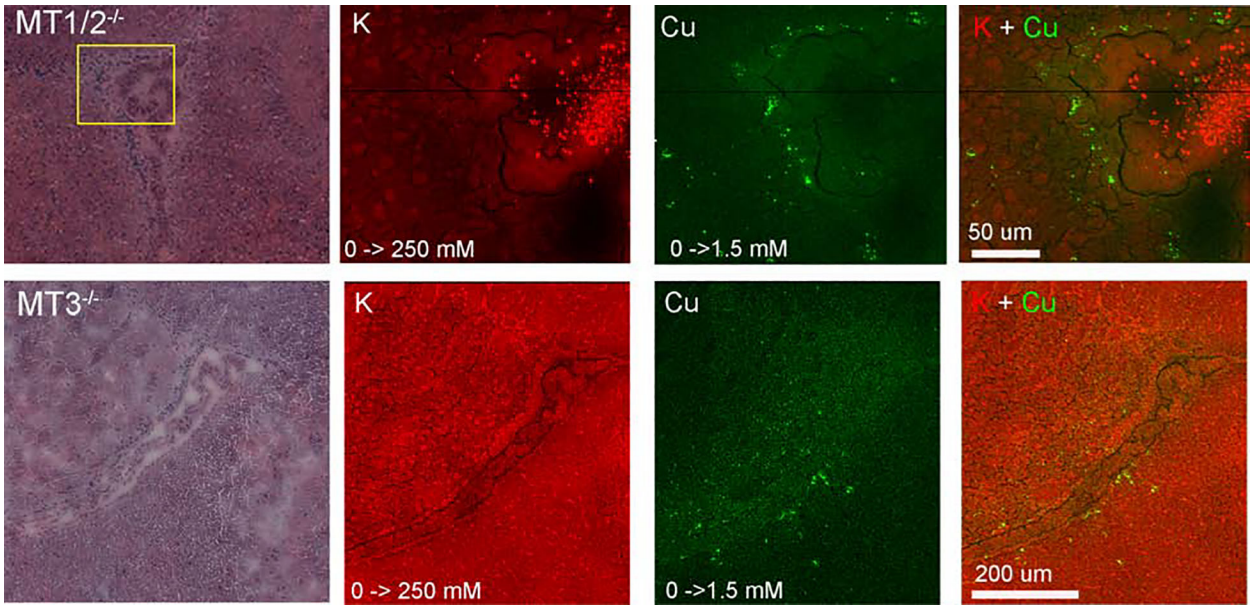

Figure 4. XFM maps and overlays for brains of different MT knockout mouse models.

H&E images, K (red), Cu (green) and overlay maps are shown for saggital sections depicting the lateral ventricle of 6-week old MT1/2$^{-/-}$ (upper) and MT3$^{-/-}$ (lower) brains Elemental concentration ranges are represented by false coloring from darkest (lowest concentration) to lightest (highest concentration). Values are shown below the individual elemental maps. Scale bars are shown in the overlay. Elemental Maps were created with MAPS [1]. Mice were provided by Dr. M Petris (University of Missouri). Unpublished results.